Synthesis, Characterization and Biological Evaluation of New Ru(II) Polypyridyl Photosensitizers for Photodynamic Therapy

Frei, Angelo ; Rubbiani, Riccardo ; Tubafard, Solmaz ; Blacque, Olivier ; Anstätt, Philipp ; Felgenträger, Ariane ; Maisch, Tim ; Spiccia, Leone ; Gasser, Gilles

Abstract: Two Ru(II) polypyridyl complexes, Ru(DIP)2(bdt) (1) and [Ru(dqpCO2Me)(ptpy)](2+) (2) (DIP = 4,7-diphenyl-1,10-phenanthroline, bdt = 1,2-benzenedithiolate, dqpCO2Me = 4-methylcarboxy-2,6-di(quinolin-8-yl)pyridine), ptpy = 4'-phenyl-2,2':6',2 -terpyridine) have been investigated as photosensitizers (PSs) for photodynamic therapy (PDT). In our experimental settings, the phototoxicity and phototoxic index (PI) of 2 (IC50(light): 25.3 M, 420 nm, 6.95 J/cm(2); PI >4) and particularly of 1 (IC50(light): 0.62 M, 420 nm, 6.95 J/cm(2); PI: 80) are considerably superior compared to the two clinically approved PSs porfimer sodium and 5-aminolevulinic acid. Cellular uptake and distribution of these complexes was investigated by confocal microscopy (1) and by inductively coupled plasma mass spectrometry (1 and 2). Their phototoxicity was also determined against the Gram-(+) Staphylococcus aureus and Gram-(-) Escherichia coli for potential antimicrobial PDT (aPDT) applications. Both complexes showed significant aPDT activity (420 nm, 8 J/cm(2)) against Gram-(+) (S. aureus; >6 log10 CFU reduction) and, for 2, also against Gram-(-) E. coli (>4 log10 CFU reduction).

DOI: https://doi.org/10.1021/jm500566f

Synthesis, Characterization and Biological Evaluation of New Ru(II) Polypyridyl Photosensitizers for Photodynamic Therapy

Angelo Frei,[a,†] Riccardo Rubbiani,[a,†] Solmaz Tubafard,[b] Olivier Blacque,[a] Philipp Anstaett,[a] Ariane Felgenträger,[c] Tim Maisch,[c] Leone Spiccia,[b] and Gilles Gasser[a,]*

[a] Department of Chemistry, University of Zurich, Winterthurerstrasse 190, CH-8057 Zurich, Switzerland; [b] ARC Centre of Excellence for Electromaterials Science and School of Chemistry, Monash University, Clayton, Victoria 3800, Australia; [c] Department of Dermatology, Regensburg University Hospital, D-93053 Regensburg, Germany.

ABSTRACT.

Two Ru(II) polypyridyl complexes, $Ru(DIP)_2(bdt)$ (**1**) and $[Ru(dqpCO_2Me)(ptpy)]^{2+}$ (**2**) (DIP = 4,7-diphenyl-1,10-phenanthroline; bdt = 1,2-benzenedithiolate; $dqpCO_2Me$ = 4-methylcarboxy-2,6-di(quinolin-8-yl)pyridine); ptpy = 4'-phenyl-2,2':6',2''-terpyridine) have been investigated as photosensitizers (PSs) for photodynamic therapy (PDT). In our experimental settings, the phototoxicity and photo-index (PI) of **2** (IC_{50}(light): 25.3 μM, 420 nm, 6.95 J/cm^2; PI: >4) and particularly of **1** (IC_{50}(light): 0.62 μM, 420 nm, 6.95 J/cm^2; PI: 80) are considerably superior compared to the two clinically approved PSs porfimer sodium and 5-aminolevulinic. Cellular uptake and distribution of these complexes was investigated by confocal microscopy (**1**) and by inductively coupled plasma-mass spectrometry (**1** and **2**). Their phototoxicity was also determined against the Gram-(+) *S. aureus* and Gram-(−) *E. coli* for potential antimicrobial PDT (aPDT) applications. Both complexes showed significant aPDT activity (420 nm, 8 J/cm^2) against Gram-(+) (*S. aureus*; >6 $\log_{10}$ CFU reduction) and, for **2**, also against Gram-(−) *E. coli* (>4 $\log_{10}$ CFU reduction).

Introduction.

Cancer has arguably been one of the most studied disease in the last 100 years. Despite enormous research efforts, cancer has caused over eight million casualties or 13% of all deaths worldwide in 2012.[1] The cornerstones of cancer therapy are radiotherapy, surgery and chemotherapy. In the search for better approaches, photodynamic therapy (PDT) has proven to be a promising new, effective and non-invasive chemotherapeutic treatment modality. The general concept of PDT is based on a photosensitizer (PS), an ideally non-toxic molecule with a higher affinity for cancer cells over healthy cells, that can be excited by irradiation with light and reach a triplet excited state through intersystem crossing. In this state, the PS can react with a substrate or solvent molecule (Type I reaction), through hydrogen atom or electron transfer, generating radicals. The PS can also transfer energy to molecular oxygen (Type II reaction), forming most prominently singlet oxygen ($^1O_2$).[2, 3] The products of these two types of reactions are highly reactive and have been shown to cause severe cellular stress and to lead to apoptosis and/or necrosis.[4-6] The advantages of PDT over other cancer therapies are the high spatiotemporal control and the low systemic toxicity of the treatment.[7] Recently, PDT has also been investigated as a new remedy against bacterial infections.[8] The application of antimicrobial PDT (aPDT) is intriguing because, unlike conventional antibiotics, aPDT does not have one specific target but instead affects multiple sites. This drastically decreases the incidence of resistance. In fact, resistance against aPDT has not been observed yet.[9, 10] With the imminent threat of widespread antibiotic resistance, aPDT could be a much needed new approach to fight the rapidly emerging, multidrug resistant superbugs. Since the approval of the first PDT drug (porfimer sodium) in 1993, multiple (13 as of 2003) PDT PSs have reached the market.[2] All of them are macrocyclic organic molecules, mostly porphyrin derivatives but also phtalocyanine-

and chlorin-based molecules.[2] These PSs share several drawbacks such as a cumbersome synthesis and purification, poor water solubility and slow clearance leading to prolonged photosensitivity in patients.[11, 12] There is therefore a need for novel PS with better photophysical and biological properties. The biological, chemical and photolytic stability are key properties of a PS for potential PDT applications. Additionally, the PS should also display a high phototoxic index (PI = ratio between toxicity in the dark and upon light irradiation), a high $^1O_2$ production quantum yield as well as being active at red-NIR wavelengths to allow for a deeper tissue penetration.

Ruthenium complexes have been under investigation for their anticancer activity for decades.[13-18] They have gained widespread attention since two complexes, namely NAMI-A and KP1019 (and the respective sodium salt KP1339), passed early clinical trials.[19-21]

The use of ruthenium in PDT however, has been quite limited so far. There have been multiple reports on porphyrin PSs decorated with ruthenium-based substituents. The resulting hybrid complexes exhibited significantly higher PIs than the individual moieties.[22-27] Charlesworth,[28] Carneiro *et al.*[29] also investigated organic PSs, phtalocyanines, conjugated to ruthenium moieties. Although the increased PIs are promising, this approach is not ideal as it requires an even longer synthetic pathway than the macrocyclic organic PSs alone. Following a similar approach, Zhou and co-workers coordinated hypocrellin B, an easily prepared phototoxic compound, to ruthenium. The resulting complex showed promising photosensitizing and photodamage properties in the red-NIR region superior to the hypocrellin B alone.[30] Another branch in the research of light-activated ruthenium complexes has investigated the ability of such compounds to release ligands and/or undergo ligand exchanges upon light irradiation. For instance Zayat,[31] Salierno and co-workers,[32] have reported complexes that release biologically

active molecules upon light irradiation. On the other hand, Sun,[33] Goldbach,[34] Wachter,[35] Sgambellone *et al*.[36] have described a series of ruthenium complexes which undergo ligand exchange and subsequent DNA binding or even cleavage upon irradiation at red-NIR wavelengths. The use of ruthenium complexes for $^1O_2$ production has gained attention only in recent years. Notably, Lincoln *et al.* have reported ruthenium polypyridyl complexes that efficiently produce $^1O_2$ upon irradiation with white light and exhibit high phototoxic indices in a metastatic melanoma model.[37] These promising, but very limited reports indicate the enormous potential of ruthenium-based PS. Still, the hitherto reported ruthenium PSs are not ideal. The conjugation of ruthenium to porphyrins does not facilitate their already cumbersome synthesis. Moreover, nuclear DNA might not be optimal target in PDT since DNA damage causes mutagenesis, which can result in resistance to further treatments.[38, 39] Hence, there certainly is still much uncharted chemical space for ruthenium PSs in PDT.

By comparison, in the realm of antibacterial research, ruthenium complexes have only sparingly been studied. There have been some reports on mono- and polynuclear Ru(II) compounds that effectively reduce the viability of different bacterial strains.[40-43] However, the field of aPDT is still in its infancy and, to our knowledge, no ruthenium PSs have been investigated for this purpose. This motivates further investigations into ruthenium complexes for antimicrobial applications. Recently, we have been applying Ru(II) polypyridyl complexes as PSs in PDT using low light doses at 350/420 nm. The studied complexes showed promising properties with regard to their $^1O_2$ yields, cellular uptake and phototoxic index.[44] Building on these promising preliminary results, we have embarked on a program to investigate in-depth the use of such complexes as PSs in PDT. Our aim is to develop biologically stable Ru(II)-based PSs

with a straight-forward synthesis and purification, high $^1O_2$ production quantum yield, high PI and possibly alternative target sites.

In the search for novel ruthenium PSs in PDT, we turned our attention to the field of dye-sensitized solar cell (DSSC). The role of ruthenium complexes in DSSCs is to absorb sunlight and inject electrons into the conduction band of an electrode.[45, 46] It has been shown that Ru(II) polypyridyl complexes perform very efficiently in DSSCs.[47-53] The complexes used for DSSCs exhibit interesting photophysical properties, such as light absorption across the visible spectrum and long excited-state lifetimes. [54-57] These properties make this class of complexes highly interesting as potential PS in PDT. Hence, with the vast number Ru(II) polypyridyl complexes that have been investigated in the field of DSSC, we decided to probe this class of complexes as PSs in PDT. It would not be the first time that metal complexes designed for a specific purpose find a novel application in a completely unrelated field. For instance, compounds originally envisioned for catalysis are being found to be promising drug candidates, e.g. Hoveyda-Grubbs catalysts demonstrated antiproliferative activity against cancer cells similar to cisplatin.[58, 59] We designed our novel, but representative complexes inspired by the work of Islam[54, 55] and Abrahamson *et al*.[56] For complex **1**, we decided to use 4,7-1,10-diphenylphenanthroline (DIP) as the polypyridyl ligand since $[Ru(DIP)_3]^{2+}$ is a known PS with a high $^1O_2$ yield (0.97 in MeOD).[60] Islam *et al.* reported that the absorbance of ruthenium complexes of the type $(Ru(\mathbf{X})_2(\mathbf{L})$, where **X** is a simple polypyridyl ligand, can be tuned by careful choice of **L** (two examples, **Ru(dcbpy)(NCS)$_2$** and **Ru(dcbpy)(bdt)** are shown in Fig. 1; dcbpy: 4,4′-dicarboxy-2,2′-bipyridine, bdt: 1,2-benzenedithiol). For bidentate dithiol ligands in particular, extensive red-shift of the complexes absorbance has reported. Based on these findings, we chose 1,2-benzenedithiol (bdt) as the third ligand due to its structural simplicity. On the other hand, for

complex **2**, we took into account the large body of research that indicated that tridentate polypyridyl ligands generally lead to broad absorption across the visible spectrum and perform inherently well in DSSC.[57, 61-64] Also in this case, relatively simple ligands were used, with only one carboxylic acid functionality present. Herein we report the synthesis and characterization of two novel Ru(II) polypyridyl PS (**1** and **2**, Fig. 1), and their phototoxic activity against human cell lines and bacterial strains.

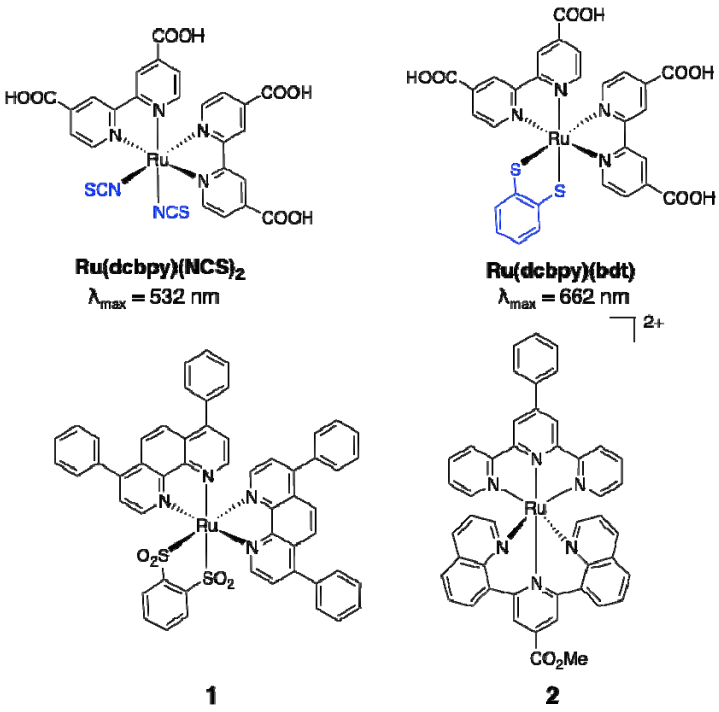

Figure 1. Structures of two representative complexes **Ru(dcbpy)(NCS)$_2$** and **Ru(dcbpy)(bdt)** reported by Islam *et al.*[54] and of the ruthenium polypyridyl complexes **1** and **2**.

Results and Discussion.

Synthesis and Characterization. The ruthenium(II) polypyridyl complex **1** was synthesized from $[Ru(DIP)_2Cl_2]$ (**1a**), which was itself obtained from $RuCl_3$ through a modified procedure reported by Caspar *et al.* (Scheme 1).[65] Due to the rapid oxidation of the sulfido ligand upon contact with air a complex mixture of products was formed preventing the isolation of **1b**. A similar observation was also reported by Begum *et al.*[66] for a related ruthenium complex. Consequently, the mixture of differently oxidized species obtained from **1b** was dissolved in acetonitrile and oxidized to the disulfinato complex **1** by addition of H_2O_2 and stirring at room temperature. After purification by column chromatography on silica, **1** could be obtained in 26% yield. The ligands, ptpy (ptpy = 4'-phenyl-2,2':6',2''-terpyridine) and dqpCO_2Me (dqpCO_2Me = 4-methylcarboxy-2,6-di(quinolin-8-yl)pyridine), were prepared according to literature procedures.[67, 68] Starting from $RuCl_3$, **2b** was obtained and used without further purification for the next step. After column chromatography on silica and subsequent counterion exchange, complex **2** was obtained as a hexafluorophosphate salt in 47% yield. For **1**, the only ESI-MS (positive mode) peak at 970.9 *m/z* could be assigned to be $[M+H]^+$ (calculated: 971.1 *m/z*). For **2**, the ESI-MS (positive mode) peak 401.0 *m/z* could be assigned to $[M]^{2+}$ (calculated: 401.1 *m/z*). Furthermore, the presence of a single major peak in the UPLC analysis and the match of the elemental analysis with <0.3% deviation unambiguously confirmed the purity of **1** and **2**.

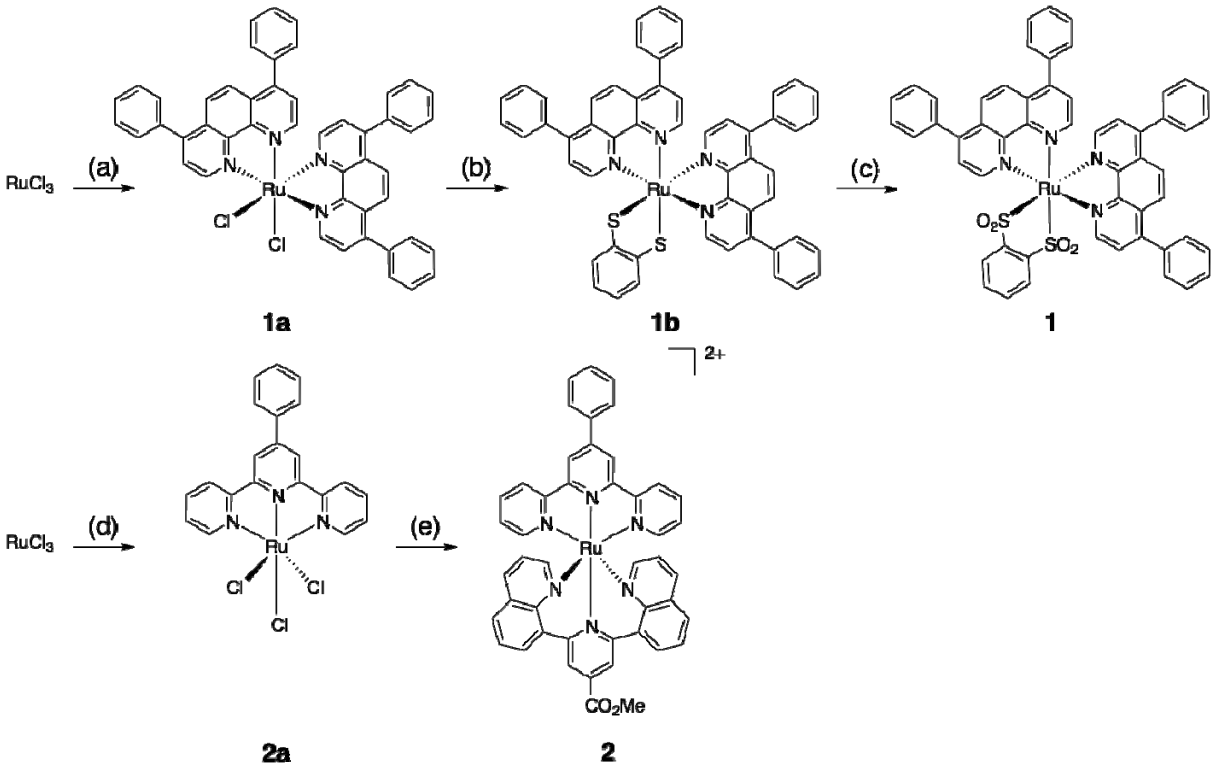

Scheme 1. Reagents and conditions: (a) 4,7-diphenyl-1,10-phenanthroline, LiCl, DMF, overnight, reflux, 50 %; (b) 1,2-benzenedithiol, EtOH overnight, reflux; (c) 30% H_2O_2(aq), CH_3CN, 30%, 48 h, r.t., 26%; (d) 4'-phenyl-2,2':6',2''-terpyridine, EtOH 3 h, reflux; (e) i) $AgBF_4$, acetone, 3 h, reflux; ii) 4-methylcarboxy-2,6-di(quinolin-8-yl)pyridine, butanol, overnight, reflux, 47 %.

X-ray Crystal Structure. Single crystals of **2** were obtained by slow evaporation of a water/acetonitrile solution (1:1 v/v). Compound **2** crystallized in the orthorhombic space group *Fdd2*. The ORTEP representation, shown in Figure 2, reveals that while the ptpy ligand is almost planar, the dqpCO_2Me ligand is strongly distorted out of the xy-plane. The Ru-N bond lengths and angles (see Table S1 in SI) are in good agreement with those for similar complexes reported in the literature.[69, 70]

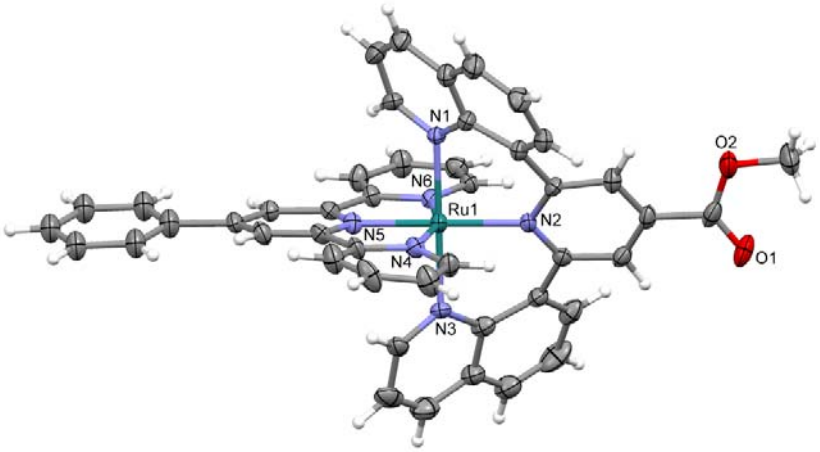

Figure 2. ORTEP representation of **2.** Ellipsoids are drawn at 20% probability level; Color code: carbon (grey), hydrogen (white).

Photophysical Properties. In order to determine if complexes **1** and **2** have properties favorable for photosensitization, a series of photophysical measurements was performed. The UV/Vis absorption and photoluminescence spectra were measured in acetonitrile (Fig. S1 in SI). From the emission spectrum of **1**, a luminescence quantum yield of 0.5% in acetonitrile could be calculated according to a standard procedure.[71] Furthermore, the luminescence lifetime was determined in both air-equilibrated (λ_{exc} = 440 nm; 189 ± 4 ns) and degassed (λ_{exc} = 440 nm; 1130 ± 28 ns) acetonitrile solutions. The results are comparable to those reported for similar Ru(II) polypyridyl complexes, indicating a phosphorescence-type emission.[72] Luminescence lifetimes in the μs-range implicate a long-lived triplet excited state, which is thought to be important for efficient photosensitization.[37] Altogether, complex **1** showed luminescence lifetimes favorable for photosensitization. The luminescence emission spectrum of **2** shows only weak intensity (Fig S1), which is reflected by a low emission quantum yield of <0.1%. The

luminescence lifetime was measured in toluene since it was below the detection limit when measured in acetonitrile. The lifetime was found to be 12 ± 2 ns under aerated conditions and 30 ± 1 ns in degassed toluene (λ_{exc} = 440 nm). These values are in agreement with those reported by Abrahamsson *et al*.[56] for similar complexes, indicating a fluorescence-type emission.

Stability in Human Plasma. In order to obtain a preliminary insight into the stability of **1** and **2** under physiological conditions, they were incubated in human blood plasma at 37 °C, following our recently developed protocol.[73, 74] No significant changes were observed either in the UV traces or in the ratio between diazepam (internal standard) and **1** and **2**, respectively, even after 48 h (Fig. 3). These results suggest that **1** and **2** are stable under physiological conditions for a therapeutically relevant time.

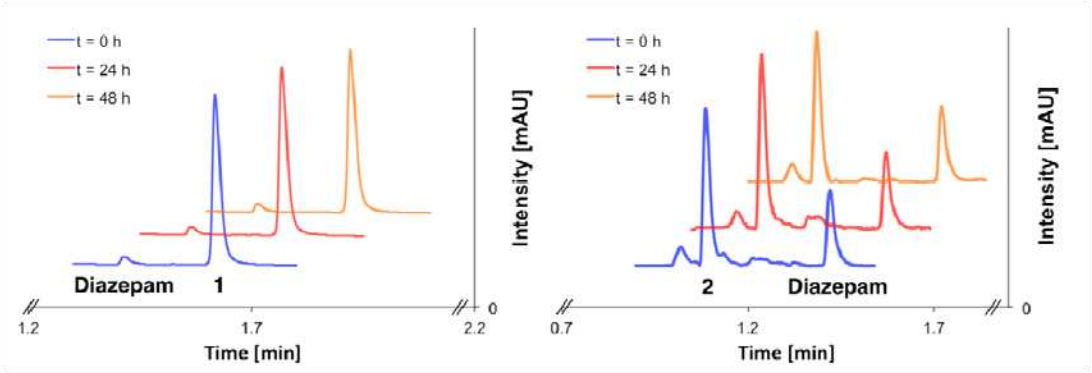

Figure 3. UV traces of UPLC analysis of **1** and **2** incubated in human plasma at 37 °C for 0 h, 24 h and 48 h using diazepam as an internal standard.

Singlet Oxygen Production. To assess the phototoxic potential of **1** and **2**, their $^1O_2$ production quantum yields (Φ_Δ) were determined in acetonitrile and phosphate buffered saline (PBS) by means of both an indirect and direct method as recently published by our group.[75] For

both methods the complexes were irradiated with 420 nm light. In the first method, $^1O_2$ production is observed indirectly through the quenching of the absorbance at 420 nm (acetonitrile) or 440 nm (PBS) of *N,N*-dimethyl-4-nitrosoaniline (RNO) by a *trans*-annular peroxide adduct formed by the reaction of $^1O_2$ with histidine in PBS. In acetonitrile, imidazole is used instead of histidine due to the low solubility of the latter in this solvent. By comparison of the quenching rates of our compounds with a reference compound (phenalenone at 420 nm) with a known $^1O_2$ production rate[76] at a given wavelength, the $^1O_2$ quantum yield of **1** and **2** could be determined in acetonitrile and PBS at an irradiation wavelength of 420 nm. It is well acknowledged that the measurement of absorbance changes are not highly sensitive.[77] To confirm the results obtained by the indirect assay, another method was employed. $^1O_2$ displays a characteristic near-IR luminescence that can be observed at 1270 nm with an IR-sensitive detector. This method could only be applied for **1** since **2** did not show a sufficiently high signal-to-noise ratio to obtain meaningful results. By comparison of the luminescence intensity measured for **1** with the one of phenalenone, a second set of $^1O_2$ quantum yields could be obtained for this complex. The measured $^1O_2$ quantum yields can be seen in Table 1. All values are expressed as the mean of three independent experiments with a standard deviation of less than 5%. Complex **1** showed an excellent $^1O_2$ production (Φ_Δ(**1**; ACN)$_{indirect}$ = 0.81; Φ_Δ(**1**; ACN)$_{direct}$ = 0.92) in acetonitrile. In PBS, both measurement techniques, direct and indirect, were at the detection limit. It is well acknowledged that singlet oxygen in aqueous solution is short-lived (≈3.5 μs) in comparison to acetonitrile (70-80 μs), which has a diminishing influence on the signal intensity.[78] The low signal-to-noise ratio did not allow an estimation with the direct method whereas the indirect method led to a low quantum yield Φ_Δ(**1**; PBS)$_{indirect}$ = 0.04). Complex **2** showed moderate $^1O_2$ quantum yields at 420 nm in acetonitrile (Φ_Δ(**2**; ACN)$_{indirect}$ =

0.15) but the direct measurement did not allow an evaluation of the quantum yield due to low signal-to-noise ratio. The different $^1O_2$ quantum yields for **1** and **2** are probably related to the difference in their luminescence lifetimes. A long luminescence lifetime indicates a long-lived triplet-excited state, which in turn is favorable for photosensitization purposes.[37] For both compounds, the highest $^1O_2$ quantum yields were measured in the more lipophilic solvent acetonitrile. Since cells do not only have polar but also lipophilic environments, compounds **1** and **2** could prove to be promising PSs.[75]

Table 1. Singlet oxygen quantum yields of **1** and **2**, values expressed as mean of three independent experiments (with standard deviation <5%).

Compound	**Solvent**	**Indirect Method** Φ_Δ**(420 nm)**	**Direct Method** Φ_Δ**(420 nm)**
1	ACN	0.81	0.92
	PBS	0.04	n.d.*
2	ACN	0.15	n.d.*
	PBS	0.03	n.d.*

*not detected

Cytotoxicity Studies. The cytotoxicity of **1** and **2** towards the human cervical cancer cell line (HeLa) was determined using a fluorometric cell viability assay (Resazurin). For comparison

purposes, the cytotoxicity of the compounds was also determined towards the human fibroblast (MRC-5) non-tumorigenic cell line with cisplatin as a reference. After 4 h incubation time, the medium was replaced with fresh medium (without complex) and the cells were irradiated at 420 nm for 15 min. The corresponding light dose (6.95 J/cm^2) is very similar to that used for the clinically approved PS porfimer sodium in comparable experiments (5 J/cm^2).[79] The IC_{50} values for all measurements are shown in Table 2. It must be noted that for the IC_{50} values determined without irradiation, two different values were obtained (for HeLa cells) for incubation times of 48 h and 4 h, respectively. This was done to compare the values with cisplatin (48 h) and with the irradiation experiments (4 h). Complex **1** shows elevated cytotoxicity against both MRC-5 and HeLa cell lines. Notably, the cytotoxicity is significantly higher against the tumorigenic cell line. Irradiation at 420 nm for 15 min increased the cytotoxicity of **1** to a remarkable IC_{50} value of 620 nM. This corresponds to a PI of 80 relative to the dark experiments. These results are even more interesting if compared to clinically established anticancer PDT agents. Under the same experimental conditions, **1** and **2** displayed a significantly higher phototoxicity and PI compared to another clinically approved PDT drug, namely 5-aminolevulinic acid (ALA),[80-82] which ist he precursor of protoporphyrin IX. Moreover, both the IC_{50} values and the PI of **1** represent a significant improvement with respect to porfimer sodium. The latter was found to have an IC_{50} value of 2.57 ± 0.12 μg/ml and a corresponding PI of >10 upon 24 h incubation in HeLa cells and irradiation with the appropriate wavelenght and a comparable light dose (5 J/cm^2) (IC_{50}(dark): >25 μg/ml; cf. values in brackets in Table 2).[79] Since cisplatin has a light-independent mode of action, the PI is not applicable for this compound.[83] Complex **2** displayed a very promising lack of activity towards non-tumorigenic cells (MRC-5) as well as towards cancerous cells (HeLa) in the dark in the range of concentrations measured in this study (up to

100 μM), while still demonstrating a moderate toxicity (IC_{50} = 25.3 ± 4.7 μM) upon irradiation and a PI of at least 4. The high phototoxicity observed for **1** upon irradiation at 420 nm is in agreement with the higher $^1O_2$ quantum yields and stronger absorption observed at this wavelength.

Table 2. IC_{50} values and phototoxic index (PI) for complexes **1** and **2**, in HeLa cancer cells and MRC-5 non-tumorigenic cells with the IC_{50} values of cisplatin as a positive control.

Compound	**MRC-5 [μM (μg/ml)] (48 h, dark)[a]**	**HeLa [μM (μg/ml)] (48 h, dark)[a]**	**HeLa [μM (μg/ml)] (4 h, dark)[b]**	**HeLa [μM (μg/ml)] (4 h, 420 nm)[c]**	**PI**
1	15.6 ± 2.7 (15.1 ± 2.6)	5.7 ± 0.7 (5.5 ± 0.7)	49.7 ± 10.1 (48.2 ± 9.8)	0.62 ± 0.28 (0.60 ± 0.27)	80
2	>100 (>100)	>100 (>100)	>100 (>100)	25.3 ± 4.7 (30.0 ± 5.6)	>4
ALA[f]	>50	>50	>50	45.5 ± 3.2	>1
Cisplatin	7.9 ± 1.2	11.5 ± 2.9	n.d.[d]	22.2 ± 5.7	n.a.[e]

[a]48 h incubation at 37 °C, 6% CO_2; [b]4 h incubation at 37 °C, 6% CO_2; [c]4 h treatment followed by 15 min irradiation at 420 nm (6.95 J/cm^2) and 44 h incubation at 37 °C, 6% CO_2; [d]not determined; [e]not applicable; [f] Measured IC_{50} values were adjusted taking into account that four molecules of ALA are required for the formation of one molecule of protoporphyrin IX, which represents the active species.[84, 85]

Cellular Localization. Having demonstrated that complex **1** possesses favorable photo-luminescence and phototoxicity properties as well as being stable under physiological conditions, its cellular localization in HeLa cells was assessed by confocal microscopy. This cell line was selected since it is considered to be a reliable and economic model for human cervical cancer. Additionally, it is also a type of cancer that is accessible by fiber-optics, which is an essential requirement for PDT applications.[86] Cells were stained with DAPI (Fig. 4a) and with the Mitotracker green FM (Fig. 4b). Complex **1** was visualized with an excitation at 400 nm (Fig. 4c), which does not interfere with the other dyes. As can be seen in Fig. 4c, the luminescence of **1** is highly visible. Fig. 4d shows the overlay of Fig 4a-4c. It can be observed that the area of the emission of **1** superimposes extremely well with the emission of the Mitotracker green FM, which localizes in mitochondria. Accumulation of the PS in the mitochondria is promising as they are important cell organelles and their damage can trigger different paths of cell death.[73, 87] We note that very poor photoluminescence of **2** precluded confocal microscopy studies.

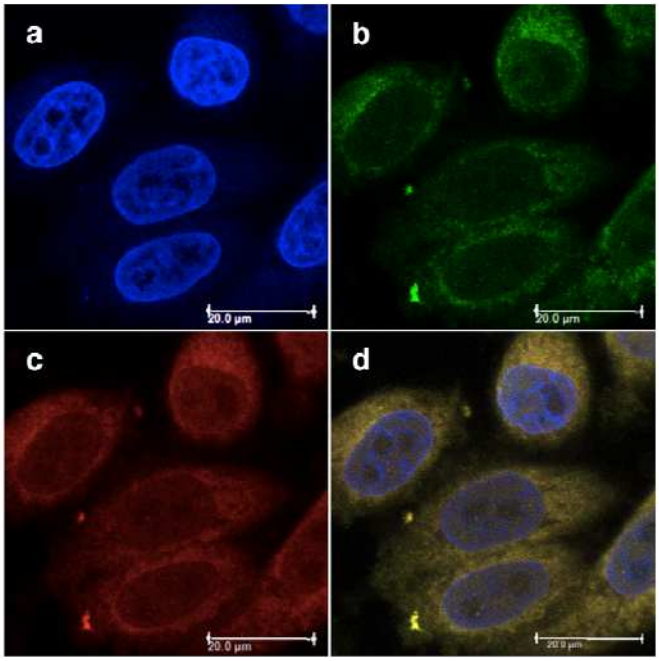

Figure 4. Fluorescence confocal microscopy images of HeLa cells incubated with 40 µM of **1** for 4 h: a) DAPI staining; b) Mitotracker green FM staining; c) visualization of 1 by excitation at 405 nm. d) overlay of a-c.

Cellular Uptake. Taking advantage of the presence of a metal in our systems, the accumulation of complexes **1** and **2** in cancer cells was investigated using inductively coupled plasma-mass spectrometry (ICP-MS). HeLa cells were incubated for different periods of time (0h, 4h and 48h) with the ruthenium compounds. **1** and **2** displayed a time dependent accumulation which is most pronounced for **1**. **1** reached a 30% higher Ru content (35.0 ng/mg protein) than **2** (23.6 ng/mg protein) after 48 h. Although **1** and **2** demonstrated considerable to high phototoxicity, it has to be acknowledged that their cellular uptake into HeLa cells is quite moderate compared to other Ru(II) complexes.[44, 88, 89]

To obtain more detailed information about the localization of **1** and **2** their subcellular accumulation was investigated. Briefly, HeLa cells were incubated with **1** and **2** for 4 h and subsequently the nuclei and mitochondria of the cells were isolated while the remaining cell material was kept as a residual fraction. The two complexes displayed a quite different cellular distribution profile (Fig. 5). For **1**, the results confirmed the data obtained by the microscopy studies with 67 % of the total Ru taken up by mitochondria (9.1 ± 1.3 ng/mg protein). We have previously observed a similarly high mitochondrial uptake with another class of Ru(II) polypyridyl complexes.[73] In contrast to the microscopy results, a significant amount of Ru could also be observed in the nuclear fraction (28%, 3.8 ± 1.3). The residual cellular fraction contained only 5% of Ru (0.7 ± 0.3 ng/mg protein). For **2**, the total ruthenium content of the isolated cell nuclei was 50 % of the total amount of up taken ruthenium (8.27 ± 0.27 ng/mg protein) while the mitochondria contained 29% (4.85 ± 0.42 ng/mg protein). The residual fraction contained 21% (3.44 ± 0.36 ng/mg protein). Taken together, these results indicate an overall moderate cellular uptake for both complexes **1** and **2**. Nevertheless, both complexes displayed significant toxicity upon light irradiation (and also in the dark for **1**) and chemical modifications (compounds (e.g. by coupling them to a targeting molecule) to improve their cellular uptake could further increase their phototoxicity.

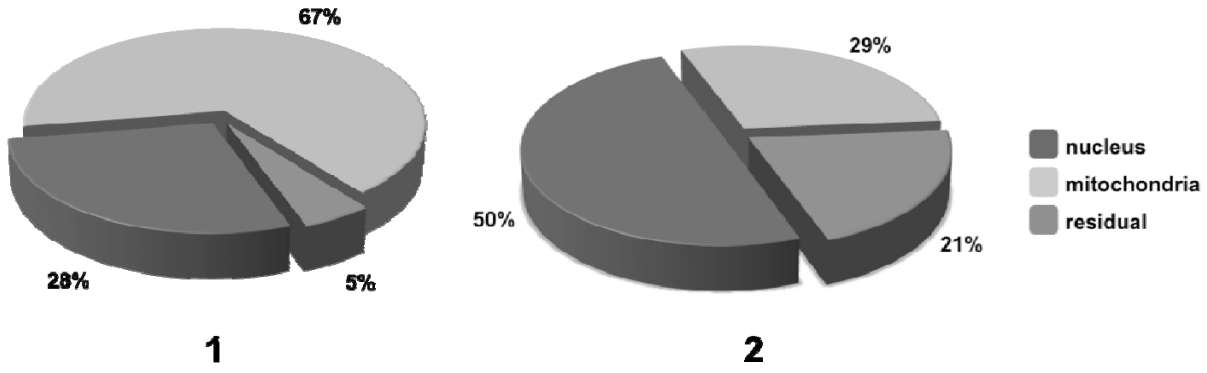

Figure 5. Ruthenium uptake in the different cellular compartments of HeLa cells treated for 4 h with 20 μM of **2** and quantified by ICP-MS.

Antibacterial Studies. To investigate the potential of complexes **1** and **2** as aPDT agents, their photoxicity was determined against two bacterial strains, the Gram-(+) *S. aureus* and the Gram-(−) *E. coli*. The efficacy of a PS in aPDT can vary substantially depending on whether the bacterial strain is a Gram-(−) or Gram-(+) species, with Gram-(−) strains being less vulnerable to certain PS.[90] The phototoxicity of **1** and **2** was determined according to a method recently published by Eichner *et al*.[91] Briefly, solutions of each bacterial strain were incubated with the respective compound for 15 min at different PS concentrations. The cells were then irradiated for 10 min with visible light (380-480 nm, λ_{max} = 420 nm, 8 J/cm^2) and the fraction of bacteria still alive was determined according to the Miles, Misra and Irwin method as the number of colony-forming units (CFU) per ml.[92] Control experiments were performed to exclude any additional toxicity by the solvent (DMSO) used to dissolve the complexes. The results are expressed as the mean of three independent experiments. In experiments where the bacteria were not irradiated, no significant change in CFU/ml was observed. For both **1** and **2**, a reduction of > 6 $\log_{10}$ (≥99.9999%) in cell viability was observed at concentrations of 50 μM (Figure 6) against the *S. aureus* strain. Considering the light dose of 8 J/cm^2 and the short incubation time used in these experiments, the results are very promising, particularly with regard to those recently reported by Schastak *et al*.[93] for a porphyrin PS. Complex **1** showed no detectable phototoxic effect against the *E. coli* strain while complex **2** reduced cell viability by > 4 $\log_{10}$ (≥99.99%) at 50 μM. This is interesting because Gram-(−) strains (like *E. coli*) are known to be less sensitive to certain types of PS. It has been reported that positively charged PS are more effective at killing Gram-(−)

bacteria and our findings are well in agreement with this hypothesis.[90] Another series of Ru(II) polypyridyl complexes was tested against *E. coli* by Lei *et al.*[94] In both cases, phototoxicty was observed but, since no light dose is reported, the results are not easily comparable. The decrease in cell viability against *S. aureus* is similar for **1** and **2**, which is in contrast to the difference in IC_{50} values observed in the HeLa cell assay. This finding can be attributed to the 16-fold longer incubation time (15 min compared to 4 h) in the human cell experiments. Also, in contrast to the procedure with the human cells, the medium was not exchanged prior to the irradiation in these experiments, thereby possibly allowing the fraction of the compound that did not enter the bacteria to also damage the cells. Both complexes showed high phototoxicity against the Gram-(+) strain *S. aureus* and **2** also effectively reduced the cell viability of the Gram-(−) strain *E. coli*. This makes **1** and particularly **2** promising candidates for aPDT applications, where topical application and irradiation wavelengths in the 400-500 nm range can be used.

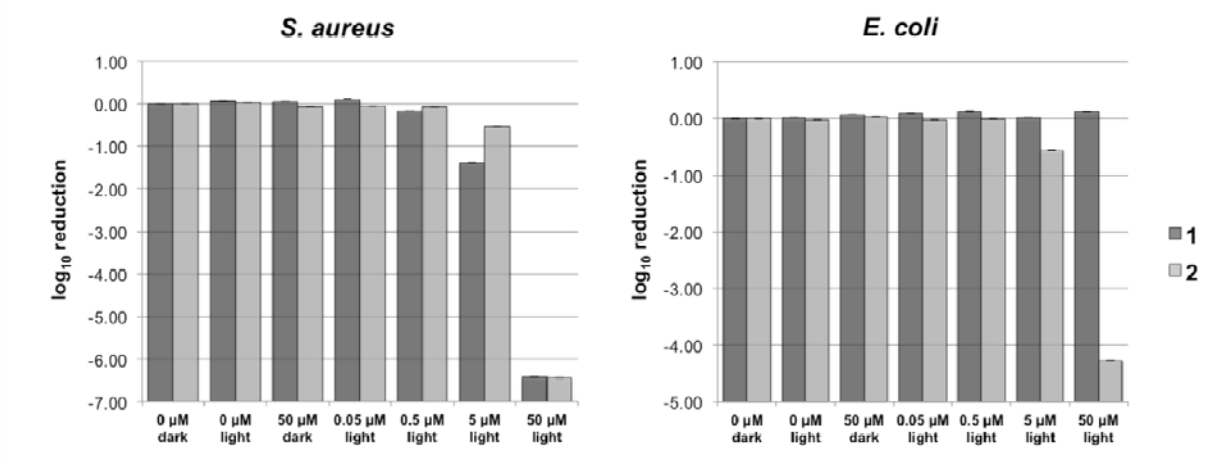

Figure 6. Antibacterial activity of complexes **1** and **2** against the two bacterial strains, *E. coli* and *S. aureus* (conditions: 15 min treatment followed by 10 min irradiation at 420 nm (8 J/cm^2) and 24 h incubation at 37 °C).

Conclusions

In a first step to probe the large library of ruthenium compounds used in DSSC in the field of PDT, two novel ruthenium(II) polypyridyl complexes (**1** and **2**) have been prepared and characterized, including by X-ray crystallography for **2**. Their stability in biological media, photophysical properties and $^1O_2$ production quantum yields have been determined. Both complexes were shown to produce $^1O_2$. Furthermore, their phototoxicity was evaluated against the human cervical cancer cell line HeLa. Complex **2** displayed phototoxicity in the low micromolar range against HeLa cells and, most importantly, no significant toxicity in dark experiments. Complex **1** showed phototoxicity in the nanomolar range with a PI of 80 against HeLa cells. This result is even more impressive when compared to the clinically approved PS ALA and porfimer sodium which display both lower phototoxicity and PIs in similar experimental settings.[79] With the help of confocal microscopy experiments, **1** was shown to accumulate in the cytoplasm, particularly in mitochondria. These results were confirmed by ICP-MS experiments, which showed an accumulation of around 67% of the total Ru taken up by the cell into the mitochondria. In comparison, the cellular uptake of **2** was shown to be quite more diffuse. In fact, **2** could be detected in all cellular compartments, with a slight preference for the cellular nucleus. Both complexes showed an overal cellular uptake 10-100 times lower than for other ruthenium complexes.[44, 88, 89] Remarkably, **2** and particularly **1** still exhibited moderate to high toxicity upon light irradiation. Improving the cellular uptake of these compounds (e.g. by coupling them to a targeting molecule) could further increase both their toxicity and selectivity against cancer cells.

In the light of the novel up-and-coming field of aPDT, the phototoxicity of **1** and **2** was also tested against the two bacterial strains *S. aureus* and *E. coli*. The former effectively reduced cell

viability in the Gram-(+) strain *S. aureus* whereas no toxicity was observed against the Gram-(−) strain *E. coli* within the experimental conditions. On the other hand, **2** effectively reduced cell viability in both, the Gram-(+) *S. aureus* and Gram-(−) *E. coli*, bacterial strains. The phototoxic profile of **2** against bacteria is particularly promising as Gram-(−) bacterial strains are reported to be inherently less affected by aPDT compared to Gram-(+) bacteria.[90] Taken together, these results further emphasize the enormous potential of ruthenium complexes in PDT and also in the nascent field of aPDT. While the wavelength of irradiation used in this work is suitable for topical applications, further work will focus on the development of novel ruthenium PS that are active in the red-NIR region, where deeper tissue penetration can be achieved.

Experimental section.

Materials. All chemicals were of reagent grade quality or better, obtained from commercial suppliers and used without further purification. The Ligands dqpCO_2Me and ptpy were prepared according to literature procedures.[67, 68] The purity of all final compounds was shown to be 95% or higher by elemental microanalysis. Solvents were used as received or dried over molecular sieves. All preparations were carried out using standard Schlenk techniques.

Instrumentation and Methods. ^{1}H and ^{13}C NMR spectra were recorded in deuterated solvents on 400 (^{1}H: 400 MHz, ^{13}C: 100.6 MHz) or 500 (^{1}H: 500 MHz, ^{13}C: 126 MHz) MHz spectrometers at room temperature. The chemical shifts, δ, are reported in ppm (parts per million). The residual solvent peaks have been used as an internal reference. The abbreviations for the peak multiplicities are as follows: s (singlet), d (doublet), dd (doublet of doublets), t (triplet), q (quartet), m (multiplet), and br (broad). ESI-MS and UPLC-MS were obtained with a Bruker Esquire 6000 mass spectrometer. LC-MS and UPLC-MS spectra were measured on an

Acquity™ from Waters system equipped with a PDA detector and an auto sampler using an ACQUITY UPLC BEH C18 Gravity 1.7 µm (2.1 × 50 mm) reverse phase column. A total of 2 µl of the solution was injected into the HPLC that was connected to a mass spectrometer operated in ESI mode The UPLC runs (flow rate: 0.6 ml/min) were performed with a linear gradient of A (acetonitrile (Sigma Aldrich HPLC-grade)) and B (distilled water containing 0.1% formic acid): t = 0−0.25 min, 5% A; t = 1.5 min, 100% A; t = 2.5 min, 100% A. Elemental microanalyses were performed on a LecoCHNS-932 elemental analyser. IR spectra were obtained with a Perkin Elmer Spectrum Two spectrometer. UV/Vis spectra were measured on a Varian Cary50Scan UV-Visible Spectrophotometer and Luminescence spectra on a Perkin Elmer LS 50 using fluorescence quartz cuvettes (width 1 cm).

Synthesis.

$Ru(DIP)_2Cl_2$: $RuCl_3$ (110 mg, 0.42 mmol), 4,7-diphenyl-1,10-phenanthroline (DIP, 266 mg, 0.8 mmol) and LiCl (100 mg, 2.36 mmol) were dissolved in DMF (10 ml). The mixture was heated to reflux overnight and then allowed to cool down to room temperature. Acetone (50 ml) was added to the solution to initialize recrystallization. The mixture was kept in the fridge for another day. The precipitate was collected by filtration and washed with diethylether (20 ml) and water (20 ml). The solid residue was dissolved in dichloromethane and collected. The solvent was removed *in vacuo* yielding a dark purple solid of $Ru(DIP)_2Cl_2$. Yield: 174 mg (50%).

The analytical data matched that reported previously.[65]

$Ru(DIP)_2(bdt)$ (1): $Ru(DIP)_2Cl_2$ (180 mg, 0.22 mmol) was dissolved in degassed EtOH (15 ml). 1,2-dimercaptobenzene (94 mg, 0.66 mmol) was added and the solution heated to reflux under nitrogen atmosphere overnight. The solvent was evaporated to dryness. The dark solid was then dissolved in dichloromethane (30 ml) and extracted with 1M $NaHCO_3$ (2x 20 ml). The

combined organic phases were dried over $MgSO_4$ and the solvent removed on a rotary evaporator. The dry dark solid was dissolved in acetonitrile (30 ml). Aqueous H_2O_2 (1 ml, 30%) was then added to the mixture. The solution was stirred under nitrogen at room temperature for 48 h. The solution was then cooled in an ice bath and MnO_2 (1.0 g, 11.5 mmol) was added to the mixture. The mixture was left standing for 30 min before it was filtered (filter paper) multiple times to remove the insoluble MnO_2. The remaining clear solution was evaporated to dryness. The resulting yellow solid was purified by column chromatography on silica (acetone/CH_2Cl_2 4:1, R_f = 0.3). The product was obtained as an orange powder. Yield: 57 mg (26%). Anal. Calcd. for $C_{54}H_{36}N_4O_4RuS_2$ (%): C, 66.86; H, 3.74; N, 5.78. Found: C, 67.02; H, 4.02; N, 5.59; IR bands (Golden Gate, cm^{-1}): ν 1559, 1428, 1141, 1052, 1005, 829, 764, 735; ^{1}H NMR (500 MHz, CD_2Cl_2): δ (ppm) 10.60 (d, ^{3}J = 5.6 Hz, 2H), 8.15−8.12 (m, 4H), 8.04−8.01 (d, 2H), 7.83−7.80 (m, 4H), 7.83−7.45 (m, 24H); ^{13}C NMR (125 MHz, CD_2Cl_2): δ (ppm) 155.54, 153.54, 151.73, 150.29, 150.14, 149.41, 148.45, 137.28, 137.00, 131.20, 130.90, 130.72, 130.33, 130.31, 130.00, 129.85, 129.18, 128.76, 126.61, 126.34, 125.99, 125.83, 120.65; MS (ESI^+): *m/z* 971.1 $[M+H]^+$, 993.3 $[M+Na]^+$. HR-ESI mass spectrum (CH_3CN + NaI): found 993.11267; calcd. for $[C_{54}H_{36}N_4NaO_4RuS_2]$ 993.11266; UV-Visible spectrum (CH_3CN): λ_{max} (ε_{max}) = 396, 440(sh) nm (26300, 19200 $M^{-1}cm^{-1}$).

Ru(dqpCO$_2$Me)(ptpy) (2). A solution containing ptpy (0.15 g, 0.50 mmol) and $RuCl_3$ (0.13 g, 0.51 mmol) in absolute EtOH (50 mL) was heated to reflux for 3 h. The solid formed was isolated by filtration, washed with EtOH (10 ml) and Et_2O (10 ml) and dried to yield the intermediate product, $[Ru(ptpy)Cl_3]$ as a red solid compound which was used directly in the next step of the synthesis. To 25 ml of acetone $[Ru(ptpy)Cl_3]$ (0.10 g, 0.21 mmol) and $AgBF_4$ (0.14 g, 0.70 mmol) were added and the mixture was refluxed for 3 h. After cooling to room temperature,

the mixture was filtered and the filtrate was evaporated to dryness on a rotary evaporator. To the residue dqpCO$_2$Me (0.78 g, 0.21 mmol) and butanol (25 ml) were added. The mixture was heated to reflux overnight. After cooling to room temperature, 1 M aqueous KPF_6 (2 ml) was added and half of the solvent evaporated on the rotary evaporator to precipitate the product, which was then collected by filtration. The obtained solid was subjected twice to flash column chromatography on silica gel (ACN: H_2O: 1M $NaNO_3$ 18:1:1 v/v/v, R_f = 0.7). The darkest red band was collected and the solvent removed under reduced pressure. The residue was suspended in acetonitrile to dissolve the complex and to separate it from the insoluble $NaNO_3$. After filtration, the ACN was removed on a rotary evaporator. The counterion was exchanged by addition of 1 M aqueous NH_4PF_6 (2 ml) and the precipitate was collected by filtration and washed with water. The product was dried *in vacuo* to yield the desired complex as a dark red powder. Yield: 110 mg, (47%). Anal. Calcd. for $C_{46}H_{32}F_{12}N_6O_2P_2Ru \cdot 3\ H_2O \cdot 1\ CH_3CN$ (%): C, 48.57; H, 3.48; N, 8.26. Found: C, 48.50; H, 3.46; N, 8.32; IR bands (neat, cm^{-1}): ν 3060, 1718, 1604, 1560, 1508, 1405, 1268, 1209, 1019, 845, 828; ^{1}H NMR (400 MHz, CD_3CN): δ (ppm) 8.74 (dd, ^3J = 7.7, 1.1, 2H), 8.72 (s, 2H), 8.61 (s, 2H), 8.35 (dd, ^3J = 8.4, 7.6, 2H), 8.27 (d, ^3J = 7.3, 2H), 8.18 (dd, ^3J = 8.1, 6.5, 2H), 8.04 (m, *w* = 11.2, 4H), 7.84 (m, *w* = 8.1, 4H), 7.68 (t, ^3J = 8.1, 1H), 7.60-7.65 (dd, ^3J = 7.9, 2H), 7.30 (dd, ^3J = 5.2, 1.4, 2H), 7.19 (m, *w* = 15.1, 2H), 6.98 (dd, ^3J =8.1, 5.2, 2H), 4.1 (s, 3H); ^{13}C NMR (400 MHz, CD_3CN): δ (ppm) 121.8, 124.1, 126.5, 127, 127.5, 127.6, 127.7, 129.2, 130.3, 132.5, 132.9, 135.7, 135.9, 138, 138.1, 138.5, 145.6, 148.6, 154.2, 154.5, 156.9, 157.4, 157.8, 52.8; ESI-MS (pos. detection mode): m/z: 401.1 $[M]^{2+}$. UV-Visible spectrum (CH_3CN): λ_{max} (ε_{max}) = 321, 362(sh), 460, 530, 570 nm (36700, 14800, 10400, 8900, 7200, $M^{-1}\ cm^{-1}$).

Singlet Oxygen Production.

***N*,*N*-Dimethyl-4-nitrosoaniline/histidine assay.** An air-saturated acetonitrile solution containing the complex (OD = 0.1 at irradiation wavelength), *N*,*N*-dimethyl-4-nitrosoaniline aniline (RNO) 24 μM, imidazole 12 mM or an air-saturated PBS buffer solution containing the complex (OD = 0.1 at irradiation wavelength), RNO 20 μM, histidine 10 mM were irradiated for different time intervals in a luminescence quartz cuvette at 420 nm in a RPR200 Rayonet Chamber Reactor (Southern New England Ultraviolet Company). The absorbance of RNO at 440/420 nm was then plotted as a function of irradiation time and the quantum yields of singlet oxygen formation (Φ_{sample}) were calculated using phenalenone (for irradiation at 420 nm) as the standard ($\Phi_{reference} = 0.95$) [76] with the formula:

$$\Phi_{sample} = \Phi_{sample} \frac{S_{sample}}{S_{reference}} \frac{I_{reference}}{I_{sample}}$$

where *S* is the slope of the absorbance vs. irradiation time and *I* is the amount of light absorption calculated as the overlap of the lamp emission spectrum and absorption spectrum of the compound according to the following formula:

$$I = \int_{\lambda} I_0[1 - 10^{-A(\lambda)}]d\lambda$$

where I_0 is the light-flux intensity of the lamp and *A* is the absorbance of the compound. In control experiments, using the same experimental conditions, phenalenone was shown to be photostable for the relevant irradiation times.

Near-IR Luminescence. Luminescence measurements were performed on a Fluorolog-3 Spectrofluorometer (JobinYvon Horiba, Model FL3-11) fitted with a 450 W xenon lamp light source and single-grating excitation and emission spectrometers. For high beam intensity, the excitation slits were set to a maximum value of 29.4 nm. A colored glass filter was placed

between the sample and the detector to cut off light below 695 nm. The emission signal was collected at right angle to the excitation path with an IR-sensitive liquid nitrogen cooled germanium diode detector (Edinburgh Instruments, Model EI-L). The detector was bias at -160V. The signal-to-noise ratio of the signal detected by the Ge-diode was improved with a lock-in amplifier (Stanford Research Systems, model SR510) referenced to the chopper frequency of 126 Hz. Data-acquisition was done with DataMax. In practice, a 20 mM stock solution of each compound dissolved in DMSO was diluted with PBS or acetonitrile (DMSO content of final solution <0.1%) to reach approximately an absorbance of 0.2 at the irradiation wavelength. This solution was then irradiated in fluorescence quartz cuvettes (width 1 cm) using a UV lamp (420 nm, slit 29.4 nm). Singlet oxygen near-IR luminescence at 1271 nm was measured by recording spectra from 1200 to 1350 nm (emission slit 5 nm, detector sensitivity 100, integration 3 (1)). The intensity of irradiation was varied via neutral density filters. Singlet oxygen luminescence peaks at different irradiation intensities were integrated and the resulting areas were plotted vs. irradiation intensities. The quantum yields were calculated by applying the formulas as used for the *N,N*-dimethyl-4-nitrosoaniline/histidine assay with phenalenone as a reference.[76]

Spectroscopic Studies. UV-Vis spectra were measured on a Varian Cary 50-Scan UV-Vis Spectrophotometer. To determine the luminescence quantum yields of the PSs, emission spectra were recorded on a Varian Cary Eclipse Fluorescence Spectrophotometer equipped with a Hamamatsu R3896 photomultiplier tube as detector, where the sample temperature can be controlled by a Peltier thermostatic system. Emission spectra were corrected for the spectral sensitivity of the detection system by standard correction curves. The emission intensities were normalized to a nominal absorption value of 0.1. Quantum yields in aerated acetonitrile were determined by comparison with the emission of $[Ru(bipy)_3]Cl_2$ in aerated water (Φ= 0.042).[71]

Luminescence lifetime measurements were recorded on an Edinburgh LP920 Laser Flash Photolysis transient absorption spectrometer using a flashlamp pumped Q-switched Nd:YAG laser (355 nm) as excitation source.

Stability in Human Plasma. The stability of the compounds in human plasma at 37 °C was evaluated following a slightly modified procedure to that recently reported by our group.[73, 74] The human plasma was provided by the Blutspendezentrum, Zurich, Switzerland. Diazepam was obtained from Sigma Aldrich (internal standard). Stock solutions of the complexes (20 mM) and diazepam (3.2 mM) were prepared in DMSO. For a typical experiment, an aliquot of the respective stock solutions and DMSO were added to the plasma solution (975 µl) to a total volume of 1000 µl and final concentrations of 40 µM for the complexes and diazepam (final concentration of DMSO < 0.5%). The resulting plasma solution was incubated for either: 0, 24 or 48 h at 37°C with continuous and gentle shaking (ca. 600 rpm). The reaction was stopped by addition of 2 ml of methanol, and the mixture was centrifuged for 45 min at 650 g at room temperature. The methanol solution was evaporated and the residue was suspended in 500 µl of 1:1 (v/v) acetonitrile/H_2O solution. The suspension was filtered and analyzed using UPLC−MS (as described in the instrumentation and methods part of this section).

X-ray Crystallography. Single-crystal X-ray diffraction data were collected at 183(2) K on an Agilent Technologies SuperNova area-detector diffractometer using a single wavelength Enhance X-ray source with Cu Kα radiation (λ = 1.5418 Å)[95] from a micro-focus X-ray source and an Oxford Instruments Cryojet XL cooler. The selected suitable single crystal was mounted using polybutene oil on a flexible loop fixed on a goniometer head and immediately transferred to the diffractometer. Pre-experiment, data collection, data reduction and analytical absorption correction[96] were performed with the program suite CrysAlisPro.[97] Using Olex2,[98] the structure

was solved by the Superflip[99] structure solution program using Charge Flipping and refined with the SHELXL2013[100] program package by full-matrix least-squares minimization on F^2. PLATON[101] was used to check the result of the X-ray analysis. Crystal Data for $C_{46}H_{32}F_{12}N_6RuP_2O_2$ (M =1091.78): orthorhombic, space group $Fdd2$ (no. 43), a = 43.6636(10) Å, b = 43.3688(7) Å, c = 9.2311(2) Å, V = 17480.4(6) Å^3, Z = 16, T = 182(2) K, μ (CuKα) = 4.489 mm^{-1}, D_{calc} = 1.659 g/mm^3, 16177 reflections measured ($5.744 \leq 2\Theta \leq 136.418$), 6703 unique ($R_{int}$ = 0.0275, R_{sigma} = 0.0308) which were used in all calculations. The final R_1 was 0.0782 ($I > 2\sigma(I)$) and wR_2 was 0.2110 (all data). The supplementary crystallographic data for this paper has been deposited with the Cambridge Crystallographic Data Centre as CCDC-990555. These data can be obtained free of charge from the Cambridge Crystallographic Data Centre via www.ccdc.cam.ac.uk/data_request/cif.

Cell Culture. Human cervical carcinoma cells (HeLa) cells were maintained in DMEM (Gibco) with 5% fetal calf serum (FCS, Gibco), 100 U/ml penicillin, 100 µg/ml streptomycin at 37°C and 5% CO_2. Normal lung fibroblasts (MRC-5) were cultured in F-10 medium (Gibco) supplemented with 10 % fetal calf serum (FCS, Gibco), 100 U/ml penicillin, 100 µg/ml streptomycin at 37°C and 5% CO_2.

Cytotoxicity Studies. Cytotoxicity studies of the effect of irradiation on human cervix HeLa cancer cell and MRC-5 non-tumorigenic cell lines treated with complexes **1** and **2** were performed by a fluorometric cell viability assay using Resazurin (Promocell GmbH). Briefly, one day before treatment cells were plated in triplicates in 96-well plates at a density of 4×10^3 cells / well in 100 µL. Upon treating cells with increasing concentrations of the ruthenium complex (complex dissolved in DMSO, concentration of DMSO < 0.5%) cells were incubated for 4 h. The medium was then replaced by fresh medium, which does not contain complexes **1** and **2** and the

plates were irradiated for 15 minutes at 420 nm (6.95 J/cm^2) or at 575 nm (6.23 J/cm^2) in a RPR200 Rayonet Chamber Reactor (Southern New England Ultraviolet Company). Upon further incubation at 37°C / 6% CO_2 for 44 h, the medium was removed, and 100 μL of complete medium containing resazurin (0.2 mg/ml final concentration) was added. After 4 h of incubation at 37 °C / 6% CO_2, the fluorescence of the highly red fluorescent resorufin product was quantified at 590 nm emission with 540 nm excitation wavelength in a SpectraMax M5 microplate Reader.

Microscopy Studies.

In Vitro Fluorescence Evaluation. Cellular localization of **1** was performed by fluorescence microscopy. HeLa cells were grown on 18 mm M enzel-Gläser coverslips in 2 ml complete medium at a density of 2.5 × 10^5 cells/ml and incubated for 2 h with **1** at 40μM (DMSO concentration < 0.5%). Cells were fixed in 4% formaldehyde solution (10% formaldehyde in 90% PBS) and mounted on slides for viewing by confocal microscopy on a CLSM Leica SP5 microscope. The ruthenium complex was excited at 456 nm and emission above 610 nm was recorded.

Nuclear and Mitochondrial Staining. Co-localization of complex **1** into the nucleus and mitochondria was examined by means of Mito-tracker green FM (Molecular Probes, excitation: 490 nm, emission: 516 nm), a mitochondria-specific dye and DAPI (excitation: 358 nm, emission: 461 nm). Briefly, a 1 mM Mitotracker Green FM stock solution made in DMSO was diluted to 10 μM working concentration in cell medium (DMEM, 5% FCS). Staining of mitochondria was accomplished by adding a 50 nM final concentration of Mito-tracker Green FM to the culture medium for the last 45 min incubation. The medium was removed and cells

were fixed in 4% formaldehyde solution before being mounted on slides added with 8 µl of DAPI (Invitrogen) for viewing by confocal microscope.

Uptake Studies.

Sample Preparation for ICP-MS.

Whole Cells. HeLa cells were seeded two days before treatment at a concentration of $1x10^6$ cells/ml in 25 cm^2 cell culture flask till 80% of confluence and incubated with the target complexes at 20 µM for 0, 4 and 48 hours (DMSO concentration < 0.1%). The medium was removed, the cells washed with PBS and trypsinized. After re- suspension in PBS, the pellet was collected by centrifugation at 5500 rpm for 4.5 minutes. Pellets were redissolved in 500 µL of PBS, lysed by a freeze-thaw cycle and treated on ultrasonic bath for 20 minutes (Digitana AG). The lysates were lyophilized on an Alpha 2-4 LD plus (CHRIST).

Cellular Fractions. HeLa cells were seeded two days before treatment at a concentration of $1x10^6$ cells/ml in 175 cm^2 cell culture flask till 80% of confluence and incubated with the target complexes at 20 µM for 4 hours (DMSO concentration < 0.1%). The medium was removed, the cells washed with PBS and trypsinized. After re-suspension in PBS, the pellet was collected per centrifugation (5910R, Eppendorf) at 500 g for 5 min at 4 °C. Mitochondria were isolated using a mitochondria isolation kit (Cat. Nr.: MITISO2, Sigma Aldrich) following the producer instructions. Briefly, the collected pellets were redissolved in 1.5 ml of lysis buffer (delivered with the kit) and allowed to react for 15 min on ice. The samples were homogenized with a pre-chilled dounce homogenizer (7 ml, tight pestle A, 30 strokes) and centrifuged at 600 g for 10 min at 4 °C. The supernatant was transferred in a fresh tube and centrifuged at 11000 g for 10 min at 4 °C. The obtained pellets represented pure mitochondrial fractions. For nucleus isolation nuclei

of HeLa cells were obtained following an established procedure with minor modifications.[102] All the fractions were isolated from the same cellular sample for direct comparative purposes. After homogenization, the pellet obtained was redissolved in 2 ml of a sucrose solution (0.25 M sucrose, 10 mM $MgCl_2$) and layered with 3 ml of a second hypertonic sucrose solution (0.35 M sucrose, 0.5 mM $MgCl_2$). The suspension was centrifuged at 1450 g and 4 °C for 5 min. The pellet was re-suspended in 3 ml of the second sucrose solution and centrifuged at 1450 g and 4 °C for 5 min to obtain the pure nuclear extract. All the steps of the isolation procedure were monitored under phase contrast microscope on Menzel-Gläser coverslips (Olympus IX81 microscope). The supernatant phases discarded during the isolation of nuclei and mitochondria procedures were collected and formed the rest fraction. An aliquot of crude lysate supernatant, nuclear, mitochondrial and rest fraction was each used for protein quantification using the Bradford method.[103] The isolated samples were lyophilized on an Alpha 2-4 LD plus (CHRIST).

ICP-MS Studies. ICP-MS measurements were performed on an Agilent QQQ 8800 Triple quad ICP-MS spectrometer (Agilent Technologies) with a ASX200 autosampler (Agilent Technologies), equipped with standard nickel cones and a "micro-mist" quartz nebulizer fed with 0.3 ml/min analytic flow (as a 2% HNO_3 aqueous solution). Ruthenium was measured against a Ru single element standard (Merck 170347) and verified by a control (Agilent5188-6524 PA Tuning 2). Ruthenium content of the samples was determined by means of a 7-step serial dilution in the range between 0 and 100 ppb in Ru (R=1.0) with a background equivalent concentration of BEC: 3.3 ppt and a detection limit of DL: 5.4 ppt. The isotope ^{101}Ru (17.06% abundance) was evaluated in "no-gas" mode. Spiking the samples with 1% methanol (to account for eventual carbon content from the biological samples) resulted in equivalent values within error ranges.

The results are expressed as ng Ru / mg protein (correction due to the different mass of the observed cellular compartments), as mean ± error of different independent experiments.

Bacteria Culture and Phototoxicity. An overnight bacteria culture (5 ml) was harvested by centrifugation (200 g, 15 min), washed with 0.01 mM phosphate-buffered saline (PBS; Biochrom, Berlin, Germany) at pH 7.4 containing 0.027 mol/l KCl and 0.14 mol/l NaCl, and suspended in PBS at an optical density of 0.6 at 600 nm, which corresponded to ~10^8 bacteria ml^{-1}, for use in the phototoxicity experiments. The bacterial suspensions were incubated with the respective PS and then irradiated using an incoherent light source (UV236, k_{em}: 380–480 nm; max 420 nm; Waldmann Medizintechnik, Villingen-Schwenningen, Germany). To minimize scattering, the 96 -well plates were exposed to the PS-bacteria suspension from the bottom of the plates. 100 µl of a bacterial suspension (*S. aureus* (atcc 25923) or *E. coli* (atcc 25922)) with a concentration of ≈ 10^8 bacteria per ml were incubated in a 96 -well plate with different PS concentrations (each 100 µl) for 15 min at room temperature under exclusion of light. Immediately thereafter, the bacteria were irradiated with a total light dose of 8 J/cm^2 (time period: 10 min). Control samples were either incubated with PS only or irradiated only without any PS incubation. After irradiation, the surviving bacteria were determined by plating out and enumeration of the colony forming units (CFU per ml). Therefore, serially diluted aliquots of treated and untreated cells were plated on Müller-Hinton agar and the number of CFU per ml was counted after 24 h at 37 °C. The method used to determine the growth of bacteria was originally described by Miles, Mirsa & Irwin.[92] A Müller-Hinton agar plate was divided into six quadrants and three drops of 20 µl each per quadrants were applied of the serially diluted suspensions. After each three drops, the pipette tips were changed. After the droplets were dried, the agar plates were inverted and incubated at 37 °C for 24 h. The day after the surviving

colonies were counted, and the three values of the respective dilution steps were summed up and an average value was calculated. A reduction of at least three orders of magnitude (i.e., 3 $\log_{10}$ units) of viable mean numbers of bacteria was stated as biologically relevant with regard to the guidelines of hand hygiene.[104]

ASSOCIATED CONTENT

Supporting Information. UV/Vis and luminescence spectra of **1** and **2**, control experiments for confocal microscopy for **1**, ^{1}H-NMR spectra of **1** and **2**, time depedent cellular uptake curves for **1** and **2** and selected bond lengths for the X-ray crystal structure of **2**. This material is available free of charge via the Internet at http://pubs.acs.org

AUTHOR INFORMATION

Corresponding Authors

* Email: gilles.gasser@aci.uzh.ch; Fax: +41 44 635 6803; Tel: +41 44 635 4630; WWW: www.gassergroup.com.

Author Contributions

†These authors contributed equally.

The manuscript was written through contributions of all authors. All authors have given approval to the final version of the manuscript.

ACKNOWLEDGMENTS

This work was financially supported by the Swiss National Science Foundation (SNSF Professorship PP00P2_133568 to G.G.), the University of Zurich (G.G.), the Stiftung für

Wissenschaftliche Forschung of the University of Zurich (G.G.), the Novartis Jubilee Foundation (R.R. and G.G.) and the Australian Research Council through the Australian Centre of Excellence for Electromaterials Science (L.S. and S.T.), the Discovery Program (L.S.) and as Discovery Outstanding Researcher Award (L.S.). The authors thank the Center for Microscopy and Image Analysis (University of Zurich) and Dr. Ferdinand Wild for the ICP-MS measurements.

ABBREVIATIONS

DIP: 4,7-diphenyl-1,10-phenanthroline, bdt: 1,2-benzenedi-thiolate, dqpCO_2Me: 4-methylcarboxy-2,6-di(quinolin-8-yl)pyridine), ptpy = 4'-phenyl-2,2':6',2''-terpyridine, PS: photosensitizer, PDT: photodynamic therapy, ICP-MS: inductively coupled plasma-mass spectrometry, ROS: reactive oxygen species, aPDT: antimicrobial PDT, PI: phototoxic index, RNO: *N*-dimethyl-4-nitrosoaniline, ACN: acetonitrile, CFU: colony-forming unit.

REFERENCES

(1) Ferlay J.; Soerjomataram I.; Ervik M.; Dikshit R.; Eser S.; Mathers C.; Rebelo M.; Parkin DM.; Forman D.; Bray F. *Cancer Incidence and Mortality Worldwide*; International Agency for Research on Cancer: Lyon, France, 2013.

(2) Dolmans, D. E. J. G. J.; Fukumura, D.; Jain, R. K. Photodynamic therapy for cancer. *Nat. Rev. Cancer* **2003,** *3*, 380-87.

(3) Foote, C. S. Definition of type I and type II photosensitized oxidation. *Photochem. Photobiol.* **1991,** *54*, 659-659.

(4) Dougherty, T. J.; Gomer, C. J.; Henderson, B. W.; Jori, G.; Kessel, D.; Korbelik, M.; Moan, J.; Peng, Q. Photodynamic Therapy. *J. Natl. Cancer Inst.* **1998,** *90*, 889-905.

(5) Yang, J. Z.; Vugt, D. A. V.; Kennedy, J. c.; Reid, R. L. Intrauterine 5-aminolevulinic acid induces selective fluorescence and photodynamic ablation of the rat endometrium. *Photochem. Photobiol.* **1993,** *57*, 803-807.

(6) Bonnett, R. Photosensitizers of the porphyrin and phthalocyanine series for photodynamic therapy. *Chem. Soc. Rev.* **1995,** *24*, 19-33.

(7) Allison, R. R.; Sibata, C. H. Oncologic photodynamic therapy photosensitizers: a clinical review. *Photodiagn. Photodyn. Ther.* **2010,** *7*, 61-75.

(8) Hamblin, M. R.; Hasan, T. Photodynamic therapy: a new antimicrobial approach to infectious disease? *Photochem. Photobiol. Sci.* **2004,** *3*, 436-450.

(9) Tubby, S. The effect of light-activated antimicrobial agents on bacterial virulence factors and key modulators of inflammation. University College London, London, 2011.

(10) Tavares, A.; Carvalho, C. M. B.; Faustino, M. A.; Neves, M. G. P. M. S.; Tomé, J. P. C.; Tomé, A. C.; Cavaleiro, J. A. S.; Cunha, Â.; Gomes, N. C. M.; Alves, E.; Almeida, A. Antimicrobial photodynamic therapy: study of bacterial recovery viability and potential development of resistance after treatment. *Mar. Drugs* **2010,** *8*, 91-105.

(11) Castano, A. P.; Demidova, T. N.; Hamblin, M. R. Mechanisms in photodynamic therapy: part one - photosensitizers, photochemistry and cellular localization. *Photodiagn. Photodyn. Ther.* **2004,** *1*, 279-293.

(12) Baas, P.; van Mansom, I.; van Tinteren, H.; Stewart, F. A.; van Zandwijk, N. Effect of N-acetylcysteine on photofrin-induced skin photosensitivity in patients. *Lasers Surg. Med.* **1995,** *16*, 359-367.

(13) Levina, A.; Mitra, A.; Lay, P. A. Recent developments in ruthenium anticancer drugs. *Metallomics* **2009,** *1*, 458-470.

(14) Bergamo, A.; Sava, G. Ruthenium anticancer compounds: myths and realities of the emerging metal-based drugs. *Dalton Trans.* **2011,** *40*, 7817-7823.

(15) Ang, W. H.; Casini, A.; Sava, G.; Dyson, P. J. Organometallic ruthenium-based antitumor compounds with novel modes of action. *J. Organomet. Chem.* **2011,** *696*, 989-998.

(16) Kilah, N. L.; Meggers, E. Sixty years young: the diverse biological activities of metal polypyridyl complexes pioneered by Francis P. Dwyer. *Aust. J. Chem* **2012,** *65*, 1325-1332.

(17) Scolaro, C.; Bergamo, A.; Brescacin, L.; Delfino, R.; Cocchietto, M.; Laurenczy, G.; Geldbach, T. J.; Sava, G.; Dyson, P. J. In vitro and in vivo evaluation of ruthenium(II)-arene PTA complexes. *J. Med. Chem.* **2005,** *48*, 4161-4171.

(18) Dougan, S. J.; Habtemariam, A.; McHale, S. E.; Parsons, S.; Sadler, P. J. Catalytic organometallic anticancer complexes. *Proc. Natl. Acad. Sci. U.S.A* **2008**.

(19) Hartinger, C. G.; Jakupec, M. A.; Zorbas-Seifried, S.; Groessl, M.; Egger, A.; Berger, W.; Zorbas, H.; Dyson, P. J.; Keppler, B. K. KP1019, a new redox-active anticancer agent – preclinical development and results of a clinical phase I study in tumor patients. *Chem. Biodiversity* **2008,** *5*, 2140-2155.

(20) Bergamo, A.; Gaiddon, C.; Schellens, J. H. M.; Beijnen, J. H.; Sava, G. Approaching tumour therapy beyond platinum drugs: Status of the art and perspectives of ruthenium drug candidates. *J. Inorg. Biochem.* **2012,** *106*, 90-99.

(21) Alessio, E.; Mestroni, G.; Bergamo, A.; Sava, G. Ruthenium antimetastatic agents. *Curr. Top. Med. Chem.* **2004,** *4*, 1525-1535.

(22) Pernot, M.; Bastogne, T.; Barry, N. P. E.; Therrien, B.; Koellensperger, G.; Hann, S.; Reshetov, V.; Barberi-Heyob, M. Systems biology approach for in vivo photodynamic therapy optimization of ruthenium-porphyrin compounds. *J. Photochem. Photobiol., B* **2012,** *117*, 80-89.

(23) Johnpeter, J. P.; Schmitt, F.; Denoyelle-Di-Muro, E.; Wagnieres, G.; Juillerat-Jeanneret, L.; Therrien, B. Photoactive sawhorse-type diruthenium tetracarbonyl complexes. *Inorg. Chim. Acta* **2012,** *393*, 246-251.

(24) Zhang, J.-X.; Zhou, J.-W.; Chan, C.-F.; Lau, T. C.-K.; Kwong, D. W. J.; Tam, H.-L.; Mak, N.-K.; Wong, K.-L.; Wong, W.-K. Comparative studies of the cellular uptake, subcellular localization, and cytotoxic and phototoxic antitumor properties of ruthenium(II)-porphyrin conjugates with different linkers. *Bioconjugate Chem.* **2012,** *23*, 1623-1638.

(25) Gianferrara, T.; Bergamo, A.; Bratsos, I.; Milani, B.; Spagnul, C.; Sava, G.; Alessio, E. Ruthenium-porphyrin conjugates with cytotoxic and phototoxic antitumor activity. *J. Med. Chem.* **2010,** *53*, 4678-4690.

(26) Davia, K.; King, D.; Hong, Y.; Swavey, S. A porphyrin-ruthenium photosensitizer as a potential photodynamic therapy agent. *Inorg. Chem. Commun.* **2008,** *11*, 584-586.

(27) Schmitt, F.; Govindaswamy, P.; Suess-Fink, G.; Ang, W. H.; Dyson, P. J.; Juillerat-Jeanneret, L.; Therrien, B. Ruthenium porphyrin compounds for photodynamic therapy of cancer. *J. Med. Chem.* **2008,** *51*, 1811-1816.

(28) Charlesworth, P.; Truscott, T. G.; Brooks, R. C.; Wilson, B. C. The photophysical properties of a ruthenium-substituted phthalocyanine. *J. Photochem. Photobiol., B* **1994,** *26*, 277-282.

(29) Carneiro, Z. A.; de Moraes, J. C. B.; Rodrigues, F. P.; de Lima, R. G.; Curti, C.; da Rocha, Z. N.; Paulo, M.; Bendhack, L. M.; Tedesco, A. C.; Formiga, A. L. B.; da Silva, R. S. Photocytotoxic activity of a nitrosyl phthalocyanine ruthenium complex - a system capable of producing nitric oxide and singlet oxygen. *J. Inorg. Biochem.* **2011,** *105*, 1035-1043.

(30) Zhou, J.; Liu, J.; Feng, Y.; Wei, S.; Gu, X.; Wang, X.; Zhang, B. Synthesis and characterization of the monomer ruthenium complex of hypocrellin B. *Bioorg. Med. Chem. Lett.* **2005,** *15*, 3067-3070.

(31) Zayat, L.; Noval, M. G.; Campi, J.; Calero, C. I.; Calvo, D. J.; Etchenique, R. A new inorganic photolabile protecting group for highly efficient visible light GABA uncaging. *ChemBioChem* **2007,** *8*, 2035-2038.

(32) Salierno, M.; Fameli, C.; Etchenique, R. Caged amino acids for visible-light photodelivery. *Eur. J. Inorg. Chem.* **2008**, 1125-1128.

(33) Sun, Y.; Joyce, L. E.; Dickson, N. M.; Turro, C. Efficient DNA photocleavage by [Ru(bpy)2(dppn)]2+ with visible light. *Chem. Commun.* **2010,** *46*, 2426.

(34) Goldbach, R. E.; Rodriguez-Garcia, I.; van Lenthe, J. H.; Siegler, M. A.; Bonnet, S. N-acetylmethionine and biotin as photocleavable protective groups for ruthenium polypyridyl complexes. *Chem. Eur. J.* **2011,** *17*, 9924-9929.

(35) Wachter, E.; Heidary, D. K.; Howerton, B. S.; Parkin, S.; Glazer, E. C. Light-activated ruthenium complexes photobind DNA and are cytotoxic in the photodynamic therapy window. *Chem. Commun.* **2012,** *48*, 9649.

(36) Sgambellone, M. A.; David, A.; Garner, R. N.; Dunbar, K. R.; Turro, C. Cellular toxicity induced by the photorelease of a caged bioactive molecule: design of a potential dual-action Ru(II) complex. *J. Am. Chem. Soc.* **2013,** *135*, 11274-11282.

(37) Lincoln, R.; Kohler, L.; Monro, S.; Yin, H.; Stephenson, M.; Zong, R.; Chouai, A.; Dorsey, C.; Hennigar, R.; Thummel, R. P.; McFarland, S. A. Exploitation of long-lived 3IL wxcited states for metal-organic photodynamic therapy: Verification in a metastatic melanoma model. *J. Am. Chem. Soc.* **2013,** *135*, 17161-17175.

(38) El-Hussein, A.; Harith, M.; Abrahamse, H. Assessment of DNA damage after photodynamic therapy using a metallophthalocyanine photosensitizer. *Int. J. Photoenergy* **2012**, 1-10.

(39) Casas, A.; Di Venosa, G.; Hasan, T.; Batlle, A. Mechanisms of resistance to photodynamic therapy. *Curr. Med. Chem.* **2011,** *18*, 2486-2515.

(40) Li, F.; Mulyana, Y.; Feterl, M.; Warner, J. M.; Collins, J. G.; Keene, F. R. The antimicrobial activity of inert oligonuclear polypyridylruthenium(ii) complexes against pathogenic bacteria, including MRSA. *Dalton Trans.* **2011,** *40*, 5032-5038.

(41) Li, F.; Feterl, M.; Mulyana, Y.; Warner, J. M.; Collins, J. G.; Keene, F. R. In vitro susceptibility and cellular uptake for a new class of antimicrobial agents: dinuclear ruthenium(II) complexes. *Journal of Antimicrobial Chemotherapy* **2012,** *67*, 2686-2695.

(42) Pandrala, M.; Li, F.; Feterl, M.; Mulyana, Y.; Warner, J. M.; Wallace, L.; Keene, F. R.; Collins, J. G. Chlorido-containing ruthenium(ii) and iridium(iii) complexes as antimicrobial agents. *Dalton Trans.* **2013,** *42*, 4686-4694.

(43) Li, F.; Harry, E. J.; Bottomley, A. L.; Edstein, M. D.; Birrell, G. W.; Woodward, C. E.; Keene, F. R.; Collins, J. G. Dinuclear ruthenium(ii) antimicrobial agents that selectively target polysomes in vivo. *Chem. Sci.* **2014,** *5*, 685-693.

(44) Mari, C.; Pierroz, V.; Rubbiani, R.; Patra, M.; Hess, J.; Spingler, B.; Schur, J.; Oehninger, L.; Ott, I.; Salassa, L.; Ferrari, S.; Gasser, G. *Chem. Eur. J.* **2014**, accepted, DOI: chem.201402796R2.

(45) Oregan, B.; Graetzel, M. A low-cost, high-efficiency solar-cell based on dye-sensitized colloidal TiO2 films *Nature* **1991,** *353*, 737-740.

(46) Nazeeruddin, M. K.; Kay, A.; Rodicio, I.; Humphry-Baker, R.; Mueller, E.; Liska, P.; Vlachopoulos, N.; Graetzel, M. Conversion of light to electricity by cis-X2bis(2,2'-bipyridyl-4,4'-dicarboxylate)ruthenium(II) charge-transfer sensitizers (X = Cl-, Br-, I-, CN-, and SCN-) on nanocrystalline titanium dioxide electrodes. *J. Am. Chem. Soc.* **1993,** *115*, 6382-6390.

(47) Jiang, K.-J.; Masaki, N.; Xia, J.-b.; Noda, S.; Yanagida, S. A novel ruthenium sensitizer with a hydrophobic 2-thiophen-2-yl-vinyl-conjugated bipyridyl ligand for effective dye sensitized TiO2 solar cells. *Chem. Commun.* **2006**, 2460-2462.

(48) Chen, C. Y.; Wu, S. J.; Li, J. Y.; Wu, C. G.; Chen, J. G.; Ho, K. C. A new route to enhance the light-harvesting capability of ruthenium complexes for dye-sensitized solar cells. *Adv. Mater.* **2007,** *19*, 3888-3891.

(49) Chen, K. S.; Liu, W. H.; Wang, Y. H.; Lai, C. H.; Chou, P. T.; Lee, G. H.; Chen, K.; Chen, H. Y.; Chi, Y.; Tung, F. C. New family of ruthenium-dye-sensitized nanocrystalline TiO2 solar cells with a high solar-energy-conversion efficiency. *Adv. Funct. Mater.* **2007,** *17*, 2964-2974.

(50) Chen, C.-Y.; Chen, J.-G.; Wu, S.-J.; Li, J.-Y.; Wu, C.-G.; Ho, K.-C. Multifunctionalized ruthenium-based supersensitizers for highly efficient dye-sensitized solar cells. *Angew. Chem. Int. Ed.* **2008,** *47*, 7342-7345.

(51) Abbotto, A.; Barolo, C.; Bellotto, L.; Angelis, F. D.; Gratzel, M.; Manfredi, N.; Marinzi, C.; Fantacci, S.; Yum, J.-H.; Nazeeruddin, M. K. Electron-rich heteroaromatic conjugated bipyridine based ruthenium sensitizer for efficient dye-sensitized solar cells. *Chem. Commun.* **2008**, 5318-5320.

(52) Vougioukalakis, G. C.; Philippopoulos, A. I.; Stergiopoulos, T.; Falaras, P. Contributions to the development of ruthenium-based sensitizers for dye-sensitized solar cells. *Coord. Chem. Rev.* **2011,** *255*, 2602-2621.

(53) Chou, C.-C.; Wu, K.-L.; Chi, Y.; Hu, W.-P.; Yu, S. J.; Lee, G.-H.; Lin, C.-L.; Chou, P.-T. Ruthenium(II) sensitizers with heteroleptic tridentate chelates for dye-sensitized solar cells. *Angew. Chem. Int. Ed.* **2011,** *50*, 2054-2058.

(54) Islam, A.; Sugihara, H.; Arakawa, H. Molecular design of ruthenium(II) polypyridyl photosensitizers for efficient nanocrystalline TiO2 solar cells. *J. Photochem. Photobiol., C* **2003,** *158*, 131-138.

(55) Islam, A.; Sugihara, H.; Hara, K.; Singh, L. P.; Katoh, R.; Yanagida, M.; Takahashi, Y.; Murata, S.; Arakawa, H. Sensitization of nanocrystalline TiO2 film by ruthenium(II) diimine dithiolate complexes. *J. Photochem. Photobiol. A* **2001,** *145*, 135-141.

(56) Abrahamsson, M.; Jäger, M.; Kumar, R. J.; Österman, T.; Persson, P.; Becker, H.-C.; Johansson, O.; Hammarström, L. Bistridentate ruthenium(II)polypyridyl-type complexes with microsecond 3MLCT state lifetimes: sensitizers for rod-like molecular arrays. *J. Am. Chem. Soc.* **2008,** *130*, 15533-15542.

(57) Medlycott, E. A.; Hanan, G. S. Designing tridentate ligands for ruthenium(ii) complexes with prolonged room temperature luminescence lifetimes. *Chem. Soc. Rev.* **2005,** *34*, 133-142.

(58) Noffke, A. L.; Habtemariam, A.; Pizarro, A. M.; Sadler, P. J. Designing organometallic compounds for catalysis and therapy. *Chem. Commun.* **2012,** *48*, 5219-5246.

(59) Oehninger, L.; Alborzinia, H.; Ludewig, S.; Baumann, K.; Wölfl, S.; Ott, I. From catalysts to bioactive organometallics: do Grubbs catalysts trigger biological effects? *ChemMedChem* **2011,** *6*, 2142-2145.

(60) DeRosa, M. C.; Crutchley, R. J. Photosensitized singlet oxygen and its applications. *Coord. Chem. Rev.* **2002,** *233-234*, 351-371.

(61) Maestri, M.; Armaroli, N.; Balzani, V.; Constable, E. C.; Thompson, A. M. W. C. Complexes of the ruthenium(II)-2,2':6',2"-terpyridine family. effect of electron-accepting and -donating substituents on the photophysical and electrochemical properties. *Inorg. Chem.* **1995,** *34*, 2759-2767.

(62) Péchy, P.; Renouard, T.; Zakeeruddin, S. M.; Humphry-Baker, R.; Comte, P.; Liska, P.; Cevey, L.; Costa, E.; Shklover, V.; Spiccia, L.; Deacon, G. B.; Bignozzi, C. A.; Grätzel, M. Engineering of efficient panchromatic sensitizers for nanocrystalline TiO2-based solar cells. *J. Am. Chem. Soc.* **2001,** *123*, 1613-1624.

(63) Barigelletti, F.; Flamigni, L.; Balzani, V.; Collin, J. P.; Sauvage, J. P.; Sour, A.; Constable, E. C.; Cargill Thompson, A. M. W. Intramolecular energy transfer through phenyl bridges in rod-like dinuclear ru(II)/os(II) terpyridine-type complexes. *Coord. Chem. Rev.* **1994,** *132*, 209-214.

(64) Medlycott, E. A.; Hanan, G. S. Synthesis and properties of mono- and oligo-nuclear Ru(II) complexes of tridentate ligands: The quest for long-lived excited states at room temperature. *Coord. Chem. Rev.* **2006,** *250*, 1763-1782.

(65) Caspar, R.; Cordier, C.; Waern, J. B.; Guyard-Duhayon, C.; Gruselle, M.; Le Floch, P.; Amouri, H. A new family of mono- and dicarboxylic ruthenium complexes [Ru(DIP)2(L2)]2+ (DIP = 4,7-diphenyl-1,10-phenanthroline): synthesis, solution behavior, and x-ray molecular structure of trans-[Ru(DIP)2(MeOH)2][OTf]2. *Inorg. Chem.* **2006,** *45*, 4071-4078.

(66) Begum, R. A.; Farah, A. A.; Hunter, H. N.; Lever, A. B. P. Synthesis and characterization of ruthenium bis-bipyridine mono- and disulfinato complexes. *Inorg. Chem.* **2009,** *48*, 2018-2027.

(67) Cave, G. W. V.; Raston, C. L. Efficient synthesis of pyridines via a sequential solventless aldol condensation and Michael addition. *J. Chem. Soc., Perkin Trans. 1* **2001**, 3258-3264.

(68) Jaeger, M.; Eriksson, L.; Bergquist, J.; Johansson, O. Synthesis and characterization of 2,6-di(quinolin-8-yl)pyridines. new ligands for bistridentate ru(II) complexes with microsecond luminescent lifetimes. *J. Org. Chem.* **2007,** *72*, 10227-10230.

(69) Cooke, M. W.; Tremblay, P.; Hanan, G. S. Carboxy-derived $(tpy)_2Ru^{2+}$ complexes as sub-units in supramolecular architectures: the solubilized ligand 42-(4-carboxyphenyl)-4,43-di-(tert-butyl)tpy and its homoleptic ru(II) complex. *Inorg. Chim. Acta* **2008,** *361*, 2259-2269.

(70) Metcalfe, C.; Spey, S.; Adams, H.; Thomas, J. A. Extended terpyridyl and triazine complexes of d6-metal centres. *J. Chem. Soc., Dalton Trans.* **2002**, 4732-4739.

(71) Ishida, H.; Tobita, S.; Hasegawa, Y.; Katoh, R.; Nozaki, K. Recent advances in instrumentation for absolute emission quantum yield measurements. *Coord. Chem. Rev.* **2010,** *254*, 2449-2458.

(72) Jenkins, Y.; Friedman, A. E.; Turro, N. J.; Barton, J. K. Characterization of dipyridophenazine complexes of ruthenium(II): the light switch effect as a function of nucleic acid sequence and conformation. *Biochemistry* **1992,** *31*, 10809-10816.

(73) Pierroz, V.; Joshi, T.; Leonidova, A.; Mari, C.; Schur, J.; Ott, I.; Spiccia, L.; Ferrari, S.; Gasser, G. Molecular and cellular characterization of the biological effects of ruthenium(II) complexes incorporating 2-pyridyl-2-pyrimidine-4-carboxylic acid. *J. Am. Chem. Soc.* **2012,** *134*, 20376-20387.

(74) Patra, M.; Ingram, K.; Pierroz, V.; Ferrari, S.; Spingler, B.; Keiser, J.; Gasser, G. Ferrocenyl derivatives of the anthelmintic praziquantel: design, synthesis, and biological evaluation. *J. Med. Chem.* **2012,** *55*, 8790-8798.

(75) Leonidova, A.; Pierroz, V.; Rubbiani, R.; Heier, J.; Ferrari, S.; Gasser, G. Towards cancer cell-specific phototoxic organometallic rhenium(i) complexes. *Dalton Trans.* **2014,** *43*, 4287-4294.

(76) Schmidt, R.; Tanielian, C.; Dunsbach, R.; Wolff, C. Phenalenone, a universal reference compound for the determination of quantum yields of singlet oxygen O2(1Δg) sensitization. *J. Photochem. Photobiol., A* **1994,** *79*, 11-17.

(77) Kiesslich, T.; Gollmer, A.; Maisch, T.; Berneburg, M.; Plaetzer, K. A comprehensive tutorial on in vitro characterization of new photosensitizers for photodynamic antitumor therapy and photodynamic inactivation of microorganisms. *BioMed Res. Int.* **2013,** *2013*, 17.

(78) Wilkinson, F.; Helman, W. P.; Ross, A. B. Rate constants for the decay and reactions of the lowest electronically excited singlet state of molecular oxygen in solution. an expanded and revised compilation. *J. Phys. Chem. Ref. Data* **1995,** *24*, 663-677.

(79) Delaey, E.; van Laar, F.; De Vos, D.; Kamuhabwa, A.; Jacobs, P.; de Witte, P. A comparative study of the photosensitizing characteristics of some cyanine dyes. *J. Photochem. Photobiol., B* **2000,** *55*, 27-36.

(80) http://fda.gov *(11.07.2014)*.

(81) Kennedy, J. C.; Pottier, R. H.; Pross, D. C. Photodynamic therapy with endogenous protoporphyrin: IX: basic principles and present clinical experience. *J. Photochem. Photobiol., B* **1990,** *6*, 143-148.

(82) Dougherty, T. J. An update on photodynamic therapy applications. *J. Clin. Laser Med. Sur.* **2002,** *20*, 3-7.

(83) Sherman, S. E.; Lippard, S. J. Structural aspects of platinum anticancer drug interactions with DNA. *Chem. Rev.* **1987,** *87*, 1153-1181.

(84) Battersby, A. R.; Fookes, C. J.; Matcham, G. W.; McDonald, E. Biosynthesis of the pigments of life: formation of the macrocycle. *Nature* **1980,** *285*, 17-21.

(85) Scolaro, L. M.; Castriciano, M.; Romeo, A.; Patané, S.; Cefalì, E.; Allegrini, M. Aggregation behavior of protoporphyrin IX in aqueous solutions: clear evidence of vesicle formation. *J. Phys. Chem. B* **2002,** *106*, 2453-2459.

(86) Muroya, T.; Suehiro, Y.; Umayahara, K.; Akiya, T.; Iwabuchi, H.; Sakunaga, H.; Sakamoto, M.; Sugishita, T.; Tenjin, Y. Photodynamic therapy (PDT) for early cervical cancer. *Cancer Chemother.* **1996,** *23*, 47-56.

(87) Newmeyer, D. D.; Ferguson-Miller, S. Mitochondria: Releasing power for life and unleashing the machineries of death. *Cell* **2003,** *112*, 481-490.

(88) Tan, C.; Wu, S.; Lai, S.; Wang, M.; Chen, Y.; Zhou, L.; Zhu, Y.; Lian, W.; Peng, W.; Ji, L.; Xu, A. Synthesis, structures, cellular uptake and apoptosis-inducing properties of highly cytotoxic ruthenium-Norharman complexes. *Dalton Trans.* **2011,** *40*, 8611-8621.

(89) Oehninger, L.; Stefanopoulou, M.; Alborzinia, H.; Schur, J.; Ludewig, S.; Namikawa, K.; Munoz-Castro, A.; Koster, R. W.; Baumann, K.; Wolfl, S.; Sheldrick, W. S.; Ott, I. Evaluation of

arene ruthenium(II) N-heterocyclic carbene complexes as organometallics interacting with thiol and selenol containing biomolecules. *Dalton Trans.* **2013,** *42*, 1657-1666.

(90) Hamblin, M. R.; Hasan, T. Photodynamic therapy: a new antimicrobial approach to infectious disease? *Photochem. Photobiol. Sci.* **2004,** *3*, 436.

(91) Eichner, A.; Gonzales, F. P.; Felgentrager, A.; Regensburger, J.; Holzmann, T.; Schneider-Brachert, W.; Baumler, W.; Maisch, T. Dirty hands: photodynamic killing of human pathogens like EHEC, MRSA and Candida within seconds. *Photochem. Photobiol. Sci.* **2013,** *12*, 135-147.

(92) Miles, A. A.; Misra, S. S.; Irwin, J. O. The estimation of the bactericidal power of the blood. *Epidemiol. Infect.* **1938,** *38*, 732-749.

(93) Schastak, S.; Ziganshyna, S.; Gitter, B.; Wiedemann, P.; Claudepierre, T. Efficient photodynamic therapy against Gram-positive and Gram-negative bacteria using THPTS, a cationic photosensitizer excited by infrared wavelength. *PLoS One* **2010,** *5*, e11674.

(94) Lei, W.; Zhou, Q.; Jiang, G.; Zhang, B.; Wang, X. Photodynamic inactivation of Escherichia coli by ru(II) complexes. *Photochem. Photobiol. Sci.* **2011,** *10*, 887-890.

(95) *Agilent Technologies (formerly Oxford Diffraction), Yarnton, Oxfordshire, England,* ***2012***.

(96) Clark, R. C.; Reid, J. S. The analytical calculation of absorption in multifaceted crystals. *Acta Crystallogr., Sect. A: Found. Crystallogr.* **1995,** *51*, 887-897.

(97) *CrysAlisPro, Version 1.171.36.20, Agilent Technologies, Yarnton, Oxfordshire, England,* ***2012***.

(98) Dolomanov, O. V.; Bourhis, L. J.; Gildea, R. J.; Howard, J. A. K.; Puschmann, H. OLEX2: a complete structure solution, refinement and analysis program. *J. Appl. Crystallogr.* **2009,** *42*, 339-341.

(99) Palatinus, L.; Chapuis, G. SUPERFLIP - a computer program for the solution of crystal structures by charge flipping in arbitrary dimensions. *J. Appl. Crystallogr.* **2007,** *40*, 786-790.

(100) Sheldrick, G. A short history of SHELX. *Acta Crystallogr. A* **2008,** *64*, 112-122.

(101) Spek, A. Single-crystal structure validation with the program PLATON. *J. Appl. Crystallogr.* **2003,** *36*, 7-13.

(102) Muramatsu, M.; Smetana, K.; Busch, H. Quantitative aspects of isolation of nucleoli of the walker carcinosarcoma and liver of the rat. *Cancer Res.* **1963,** *23*, 510-518.

(103) Bradford, M. M. A rapid and sensitive method for the quantitation of microgram quantities of protein utilizing the principle of protein-dye binding. *Anal. Biochem.* **1976,** *72*, 248-254.

(104) Boyce, J. M.; Pittet, D. Guideline for hand hygiene in health-care settings: recommendations of the healthcare infection control practices advisory committee and the hicpac/shea/apic/idsa hand hygiene task force. *Am. J. Infect. Control* **2002,** *30*, S1-S46.

TOC Figure.

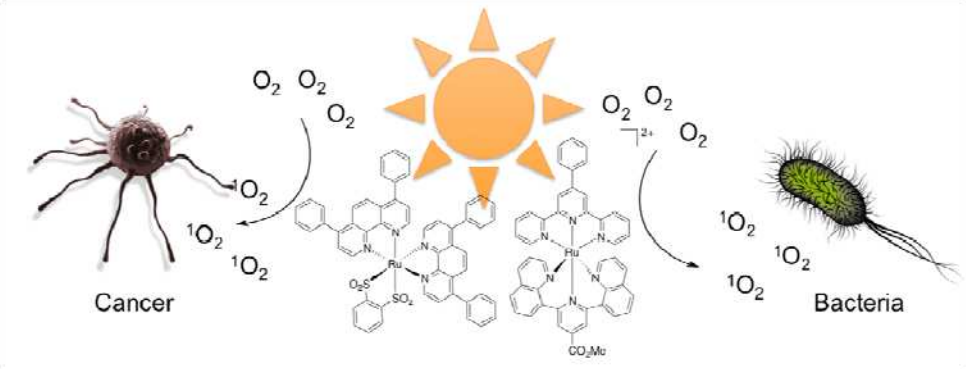
O2 O2 O2
O2 O2 O2
1O2
1O2
1O2
1O2
1O2
1O2
Cancer
Bacteria
Ru
Hu
SO2
CO2Me